Quinoline ATP Synthase Inhibitors with Activity Against Multidrug Resistant *Acinetobacter baumannii* and *Pseudomonas aeruginosa*

Katie T. Ward[+],[b] Alexander P. L. Williams[+],[b] Angelina L. Dennison[+],[b] Lena Aamir,[b] Darien L. Allen,[b] Britza Chavez-Arellano,[b] Toni A. Marchlewski,[b] Mars L. Zappia,[b] Amanda L. Wolfe,*[a] and P. Ryan Steed*[a]

The Gram-negative, pathogenic bacteria *Acinetobacter baumannii* (AB) and *Pseudomonas aeruginosa* (PA) have been identified as a particular threat due to rising multidrug resistance, and antibiotics with novel mechanisms of action are needed. Bacterial bioenergetics is a promising but underdeveloped drug target since the complexes of oxidative phosphorylation are critical to cell survival in these organisms. Building from our previous work using quinoline derivatives to inhibit the ATP synthase of PA, we report a new set of 14 quinoline derivatives that demonstrates potent inhibition of the AB ATP synthase, with the best inhibitor having an IC50 of 230 ng/mL *in vitro*, expands the quinoline structure-activity relationship against the PA enzyme, and establishes molecular strategies for achieving selectivity between PA and AB. Furthermore, several compounds demonstrated potent antibacterial activity against multidrug resistant strains of AB and PA indicating ATP synthase as a promising new area for broad spectrum antibiotic development in AB.

Introduction

Multidrug-resistant (MDR) bacterial pathogens are a growing public health threat that caused or have been associated with nearly 5 million deaths globally in 2021 and are forecast to increase to over 8 million per year by 2050, disproportionately affecting children and the elderly.[1] While infections caused by MDR bacteria were declining in the US in 2019, the United States' Centers for Disease Control and Prevention (CDC) reports that the COVID-19 pandemic caused an increase in hospital acquired infections (HAIs) by more than 20%, with resistant Enterobacteralus, *Acinetobacter* spp., *Staphylococcus aureus* (SA), *Pseudomonas aeruginosa* (PA), *Enterococcus* spp., and *Candida aureus* pathogens driving the increase.[2,3]

[a]   Dr. A. L. Wolfe, Dr. P. R. Steed
      Chemistry and Biochemistry
      University of North Carolina Asheville
      One University Heights, Asheville NC 28804
      E-mail: psteed@unca.edu
            awolfe@unca.edu

[b]   K. T. Ward,+ A. P. L. Williams,+ A. L. Dennison,+ L. Aamir, D. L. Allen,
      B. Chavez-Arellano, T. A. Marchlewski, M. L. Zappia
      Chemistry and Biochemistry
      University of North Carolina Asheville
      One University Heights, Asheville NC 28804

[+]   These authors contributed equally to this work.

🖳   Supporting information for this article is available on the WWW under
      https://doi.org/10.1002/cmdc.202400952

Acinetobacter baumannii (AB), a Gram-negative, biofilm forming bacterium, is a common cause of HAIs stemming from central line-associated bloodstream infections, catheter-associated urinary tract infections, and surgical site infections. Currently the CDC's Antimicrobial Resistance and Patient Safety Portal, a database for the rate of MDR HAIs, shows that 41% of HAIs caused by *Acinetobacter* species in the United States are MDR, and 39.5% are specifically carbapenem resistant.[2] Carbapenem resistant AB, specifically, has been designated an "Urgent Threat" by the CDC.[3] In addition to being resistant to carbapenem antibiotics, MDR AB strains have been found to have resistance to cephalosporins, quinolones, fluoroquinolones, aminoglycosides, and piperacillin.[4,5] Polymixins are currently used clinically to treat MDR AB infections, but they pose a significant toxicity risk to patients.[5]

Despite the rise in AB infections, no new classes of antibiotics to treat AB, or Gram-negative pathogens broadly, have been developed since 1968 due to the challenges of treating these pathogens. Specifically, Gram-negative bacteria possess a difficult-to-penetrate outer membrane (OM), which reduces antibiotic accumulation in the cell compared to Gram-positive bacteria like SA, in addition to common molecular resistance mechanisms like target modification, antibiotic modifying enzymes, and upregulation of efflux pumps.[4–6] To circumvent established resistance mechanisms, new cellular targets need to be explored for antibiotic development.

Bacterial bioenergetic systems have recently emerged as potential targets for antibiotic development, especially ATP synthase, given their centrality in cellular processes and survival.[7,8] AB is strictly aerobic and thus requires oxidative phosphorylation for survival,[9,10] and PA, while able to grow anaerobically, still requires a functional electron transport chain and ATP synthase.[11,12] Bacterial F_1F_o ATP synthases are multi-

ChemMedChem

Research Article
doi.org/10.1002/cmdc.202400952

**Chemistry
Europe**
European Chemical
Societies Publishing

meric complexes (Figure 1A) that use the electrochemical proton gradient formed by respiratory complexes in the cell membrane to drive synthesis of ATP from ADP and phosphate using a H^+-driven rotary catalytic mechanism.[13] H^+ enters the membrane-embedded F_o sector via subunit *a* and protonates a conserved acidic residue (Asp60 in AB, Figure 1B) in each *c* subunit of the homo-oligomeric *c*-ring. This protonation event and subsequent release of H^+ into the cytoplasm drives rotation of the c-ring, which in turn drives the conformational cycle in F_1 catalyzing ATP synthesis. The quinoline-derived, clinically-approved drug bedaquiline (BDQ) inhibits *Mycobacterium tuberculosis* (MT) ATP synthase by binding to the conserved *c*Glu65, which in turn halts the rotary mechanism, depleting cellular ATP and leading to cell death.[14,15] While there are multiple binding sites for BDQ around the *c*-ring, the highest affinity site is likely the "leading" site at the edge of the subunit *a-c* interface, where BDQ makes contacts with adjacent *c* subunits and subunit *a*.[15] The success of BDQ has made ATP synthase a promising target for antibiotic development, especially in Gram-negative pathogens, like AB and PA, that are increasingly resistant to current antibiotics.

Previously, we synthesized and evaluated a series of C1/C2 quinoline analogs that inhibited PA ATP synthase *in vitro* and inhibited growth of MDR PA.[17–19] Of the analogs synthesized, **WSA236** and **WSA238** (Figure 1C) were found to be the most potent PA ATP synthase inhibitors with IC_{50} values of 1 μg/mL

(2 μM) against PA ATP synthase expressed in *Escherichia coli* (EC) and MICs of 16–64 μg/mL against MDR PA cells. From this previous work, we found that a benzyl sulfide at C1 and a flexible side chain with a basic nitrogen (NH^+ $pK_a > 5$) approximately 9 Å from quinoline at C2 balanced high potency against ATP synthase and the ability to penetrate the OM of PA.[19] Given the high similarity of AB ATP synthase to the PA enzyme, especially in the quinoline binding site (Figure 1D), we sought to characterize the potency of existing and novel quinoline inhibitors against MDR AB while also expanding the structure activity relationship (SAR) study of quinoline inhibitors of PA ATP synthase. Herein, we detail the synthesis and evaluation of 14 novel quinoline analogs derived from **WSA236** and **WSA238**, resulting in quinolines that are effective inhibitors of AB ATP synthase, have antibiotic activity against MDR AB, and show increased potency against PA.

Results and Discussion

Synthesis

To identify inhibitors of AB ATP synthase, as well as expand the structure activity relationship (SAR) profile of quinoline derivatives against PA ATP synthase, we synthesized a series of benzyl sulfide quinoline C2 (east)/C6-C8 (west) derivatives. First, three
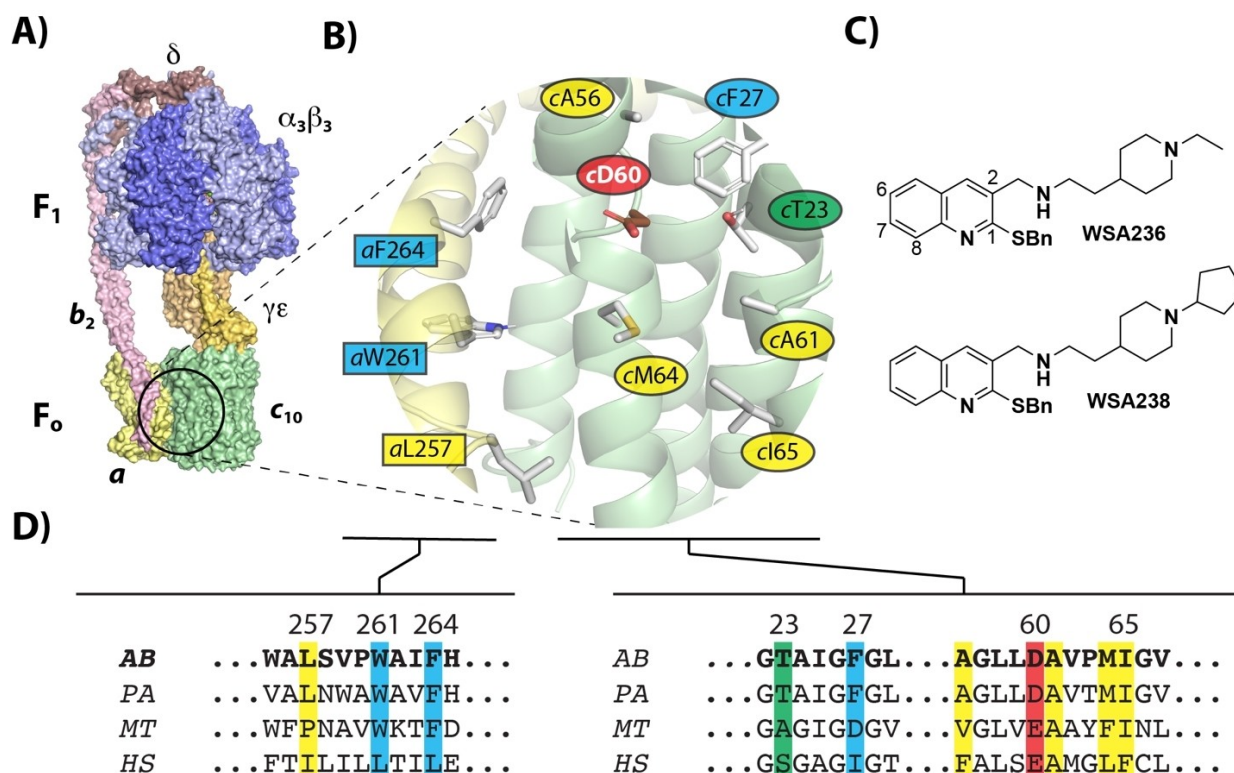

Figure 1. A) The structure of AB F_1F_o ATP synthase determined by cryo-EM (PDB ID: 7P2Y).[16] B) Detail of the putative quinoline binding site centered around Asp60 (brown) on subunit c with contributions from other residues from subunit a (pale yellow) and subunit c (pale green). C) Structures of previously reported quinoline-derived inhibitors of PA ATP synthase. Key positions on the quinoline backbone are numbered. D) Segments of the amino acid sequences of subunit a (left) and subunit c (right) that contribute to the putative quinoline binding site are aligned to compare AB with PA, MT, and *Homo sapiens* (HS). The critically conserved Asp60 is highlighted in red. Other potential interactions include aliphatic (yellow), aromatic (blue), and polar (green) residues.

ChemMedChem

Research Article
doi.org/10.1002/cmdc.202400952

**Chemistry
Europe**
European Chemical
Societies Publishing

additional C2 amines were synthesized to establish if antibiotic activity against AB was also driven by amine basicity using the same synthetic approach as previously reported for PA.[19,20] Briefly, starting from commercially available 2-chloroquinoline-3-carbaldehyde (**1**) nucleophilic aromatic substitution (NAS) afforded 2-(benzylthio)quinoline-3-carbaldehyde (**4**) in moderate yield (Scheme 1A). Reductive amination of **4** with (4-(piperidin-1-yl)phenyl)methanamine, (4-(pyrrolidin-1-ylmethyl)phenyl)methanamine, or 2-(4-methylpiperazin-1-yl)ethan-1-amine then provided **WSA248**, **WSA249**, and **WSA250** respectively (Scheme 1A).

To explore the effects of modifications on the western side of the quinoline core, two series were synthesized. Trimethoxy quinolines **WSA251**, **WSA252**, and **WSA253** were synthesized using the same approach as the original series starting from commercially available 2-chloro-6,7,8-trimethoxyquinoline-3-carbaldehyde (**2**, Scheme 1A). C6 phenyl quinolines **WSA261**, **WSA262**, **WSA269**, and **WSA270** were synthesized starting from 2-chloro-8-bromoquinoline-3-carbaldehyde (**3**),[21] which first underwent NAS to provide **6** (Scheme 1A) in moderate yield. Then reductive amination of **6** with 2-(1-ethylpiperidin-4-yl)ethan-1-amine, 2-(1-cyclopentylpiperidin-4-yl)ethan-1-amine, (4-(pyrrolidin-1-ylmethyl)phenyl)methanamine, or 2-(4-methyl-piperazin-1-yl)ethan-1-amine provided brominated quinolines **WSA254**, **WSA255**, **WSA256**, and **WSA257** respectively. Finally, a Suzuki coupling between the brominated quinolines and phenylboronic acid provided C6 phenyl quinolines **WSA261**, **WSA262**, **WSA269**, and **WSA270** (Scheme 1B).
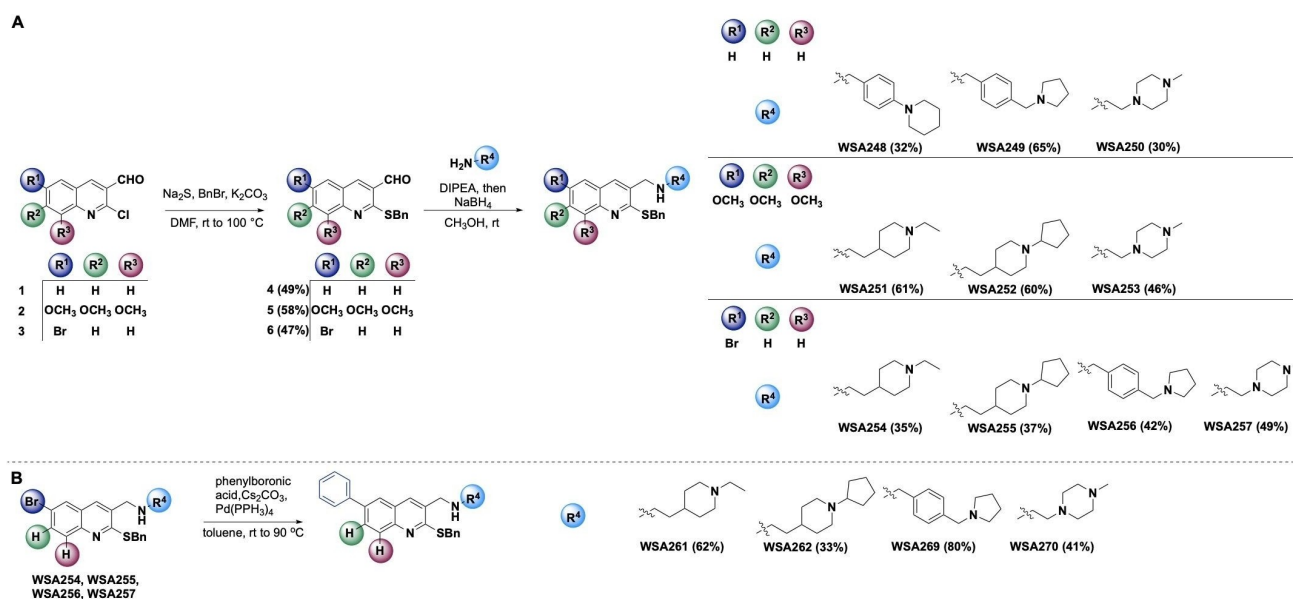
ATP Synthase Inhibition

We evaluated the above compounds for inhibition of ATP synthesis activity in inverted inner membrane vesicles (no outer membrane) prepared from AB or PA. Briefly, the native electron transport chains in the vesicles were energized using NADH, and resulting ATP synthesized was detected using a previously reported luciferin/luciferase assay.[18] Gradient-dependent ATP synthesis activity in AB vesicles was linear over the 10 min assay period and specific activity under these conditions was 8.4 ± 0.7 nmol/min/mg (Figure S1). Relative activities in the presence of increasing concentrations of tested compounds were fit with a dose-response curve to determine IC_{50} values for each compound. Representative dose response curves showing inhibition of AB ATP synthase activity are plotted in Figure 2, and all ATP synthesis inhibition data and fits are plotted in Figures S2 and S3. IC_{50} values and Hill coefficients resulting from the fit are plotted in Figure 3 for comparison.

In general, compounds were more potent against AB ATP synthase, with the most potent inhibitors being **WSA238** ($IC_{50} =$ 220 ng/mL), **WSA255** ($IC_{50} =$ 120 ng/mL), and **WSA257** ($IC_{50} =$ 120 ng/mL) (Figure 3A and Table S1). For PA, the most potent inhibitors were compounds **WSA236** ($IC_{50} =$ 520 ng/mL), **WSA255** ($IC_{50} =$ 230 ng/mL), and **WSA257** ($IC_{50} =$ 130 ng/mL) (Figure 3A and Table S1). Of the compounds tested, only **WSA248** showed no significant inhibition of either AB or PA, even at high concentrations (Figs. S2 and S3).

Across the C2 analogs of the unmodified quinoline core, where R^1-R^3 are hydrogens (**WSA236**, **WSA238**, **WSA248**, **WSA249**, **WSA250**), analogs with bulkier basic amines (**WSA236**, **WSA238**, and **WSA249**) showed greater inhibition of both AB and PA ATP synthase compared to the bulky but less basic N-phenylpiperidine (**WSA248**) and the smaller but more basic piperazine (**WSA250**). This trend is consistent with our previously reported series of PA ATP synthase inhibitors, where larger C2 amines where generally more potent.[19] Additionally, Hill slopes across the C2 series tended to be less than one for inhibition of AB ATP synthase (Figure 3B), suggesting a second inhibitor binding site that is lower affinity and/or less sensitive to inhibition. The existence of multiple binding sites for

Scheme 1. Synthesis of quinoline compounds.

ChemMedChem

Research Article
doi.org/10.1002/cmdc.202400952

Chemistry
Europe
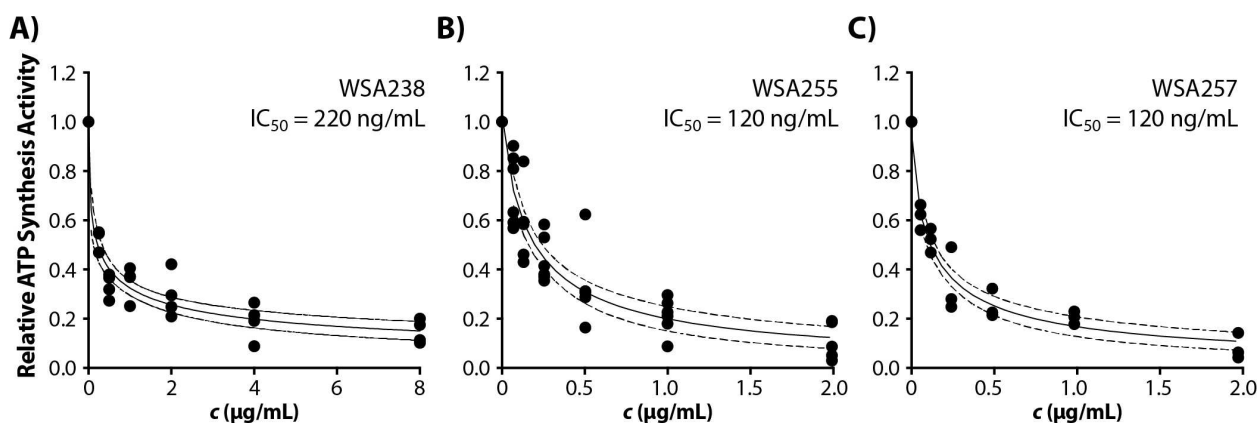European Chemical
Societies Publishing

Figure 2. Inhibition of AB ATP synthesis activity in inner membrane vesicles by the most potent compounds: WSA238 (A), WSA255 (B), and WSA257 (C). Individual data points ($n \geq 3$) were fit with a variable slope dose response curve (solid line). Dashed lines indicate the 95% confidence bands for the fit.
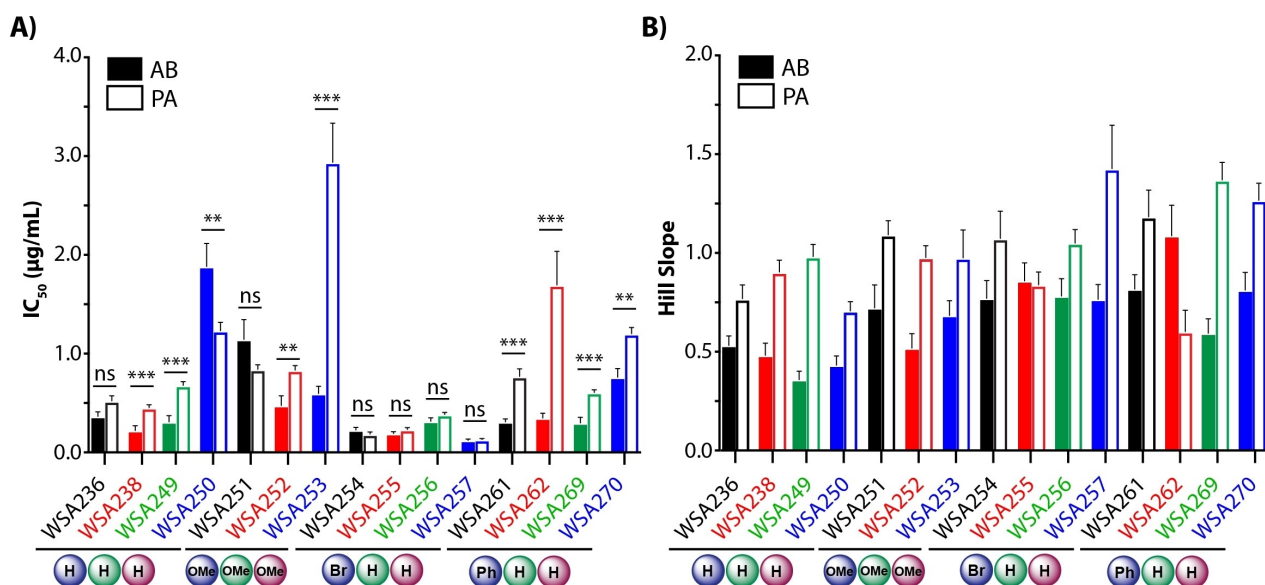

Figure 3. Comparison of potency against AB and PA ATP synthase. A) IC_{50} values from dose response fits are plotted for AB (filled bars) and PA (open bars) ATP synthase inhibition. Compounds are grouped by western modification and colors correspond to the C2 amine (*black*, *N*-ethyl piperidine; *red*, *N*-cyclopentyl piperidine; *green*, benzyl pyrrolidine; *blue*, *N*-methyl piperizine). Error bars represent standard error of the IC_{50} parameter of the fit, and statistically significant differences between AB and PA are marked (ns, $p > 0.05$; **, $p \leq 0.01$; ***, $p \leq 0.001$). B) Hill slopes from dose response fits are plotted for AB (filled bars) and PA (open bars) ATP synthase inhibition and colored as in panel A. Error bars represent standard error of the Hill parameter of the fit. WSA248 is omitted from these plots due to its low potency.

quinoline inhibitors is well supported by previous structural studies of MT ATP synthase,[15,22] which identified three unique sites with varying affinity for BDQ binding, including multiple identical sites at each lipid-exposed Asp60 in the *c*-ring. Hill slopes for inhibition of PA ATP synthase tended to be approximately one, suggesting that one particular binding site is much higher affinity than others. In general, modifications on the western side of quinoline increase the Hill slope, suggesting that addition of these groups increase selectivity for a single site on the enzyme.

SAR on the western side of quinoline also appears to follow steric bulk, where potency increases with molecular weight up to a limit. The addition of bromine on the western side of quinoline ($R^1 = Br$) increased potency of the two smaller C2 amines against AB ATP synthase and increased potency of all

amines against PA (Figure 3A). For the larger C2 amines, addition of methoxy or benzyl groups on the western side of quinoline has negligible or detrimental effects on potency, which could indicate that quinolines that already have larger substituents no longer fit in the binding site when the additional bulk is added. Interestingly, western modifications did improve potency with methylpiperizine, the smallest of the tested C2 amines, but only against AB ATP synthase. **WSN250**, which has no western modification (R^1-$R^3 = H$), was more potent against PA than AB. However, addition of trimethoxy (**WSN253**) or benzyl (**WSN270**) modifications on the western side switched selectivity so that these compounds were more potent against AB than PA. In the case of the trimethoxy modification, this difference was most pronounced, with modification improving IC_{50} by 3-fold for AB and worsening IC_{50} by nearly 3-fold for PA.

ChemMedChem

Research Article
doi.org/10.1002/cmdc.202400952

Chemistry Europe
European Chemical
Societies Publishing

Overall, results from this series suggest that AB ATP synthase may be able to better accommodate increased steric bulk on the western side of the quinoline that cannot be accommodated as well by the PA enzyme. The only significant difference in amino acid sequence at the expected quinoline binding site on subunit *c* is at position 63 (AB numbering), which is Pro in AB and Thr in PA. This difference may alter the positions of hydrogen bonding groups and affect the kinked shape of the α-helices that form the binding site. The results indicate that these differences could be explored further in the future to make highly selective inhibitors. Indeed BDQ, which has nanomolar potency against MT ATP synthase,[15] does not fully inhibit AB or PA ATP synthase even at the highest concentrations tested here (Figure S4), further demonstrating that achieving species selectivity with quinolines is possible.

Electron Transport Chain Inhibition

Given the reliance of the ATP synthesis assay on the activity of the intrinsic electron transport chain (ETC) present in inverted membrane vesicles, we tested whether the inhibitor compounds also target the ETC. To establish whether these inhibitors were selective for ATP synthase over the ETC, inhibition of the PA and AB ETC was measured for each inhibitor as previously described.[17–19] Briefly, dehydrogenase complexes were energized with NADH to initiate redox-driven H^+ pumping into the vesicle lumen, which was in turn detected by the quenching of 9-amino-6-chloro-2-methoxyacradine (ACMA) fluorescence. Most compounds were tested at concentrations of 2 μg/mL and 32 μg/mL to establish whether ETC inhibition occurred in the same range as ATP synthase inhibition (Figure S5). For any compounds that significantly inhibited the ETC at low concentration ($\geq$ 50% inhibition at 2 μg/mL), IC_{50} values were determined using a broader range of inhibitor concentrations (Table S1, Figure S5). While nearly all analogs inhibited AB and PA ETC at high concentrations (32 μg/mL), even the most potent PA ETC inhibitor, **WSA255**, which had an IC_{50} of 1.7 μg/mL against PA ETC, was more than 7-fold less potent against the ETC compared to ATP synthase. Therefore, we conclude that this series of inhibitors is selective for ATP synthase, but an unidentified complex in the ETC is a secondary target for some inhibitors (esp. **WSA254**, **WSA255**, and **WSA257**). Identifying this secondary target will require further work, as the ETC assay used here does not discriminate among several possible modes of ETC inhibition, including binding to one or more respiratory complexes or possibly acting as an ionophore. Pursuing such "dual action" inhibitors would be potentially advantageous with further development since bacteria would be slower to acquire resistance in both targets.[23]

Antibacterial Activity

To evaluate antibiotic potential of each analog compared to lead compounds **WSA236** and **WSA238**, a broth microdilution antibacterial activity assay was conducted against clinical isolate strains of AB (17978 and 1605) and PA (2108), including one MDR strain of each species: AB BAA-1605, resistant to Aztreonam, Cefepime, Ceftazidime, Ciprofloxacin, Gentamicin, Imipenem, Meropenem, Piperacillin, and Ticarcillin,[24] and PA BAA-2108, resistant to Imipenem, Meropenem, and Tobramycin.[25] Analogs were also tested against susceptible strains of *Escherichia coli* (EC) and *Staphylococcus aureus* (SA) to begin establishing the breadth of activity.

The most potent analogs overall against AB, with MICs between 8–16 ug/mL against one or both strains tested, were **WSA254**, **WSA255**, **WSA257**, **WSA261**, and **WSA270** (Table 1). Across the series, antibacterial activity against MDR PA was generally less, with the exception of **WSA249**, which along with **WSA257**, were the most potent analogs against MDR PA with MICs of 16 ug/mL. Analogs **WSA248**, **WSA256**, and **WSA269** were inactive against all AB and PA strains at the highest concentration tested. All analogs were either equipotent or less potent against the susceptible strains of EC and SA compared to AB and PA (Table S2) except for **WSA261**, **WSA262**, and **WSA270**, which were slightly more potent (down to 4 μg/mL against SA). The differences observed in MICs across bacterial species is promising in that it suggests these compounds are not universally toxic, though they will likely require additional development to improve their toxicity profile against human cells (Table S3).

Table 1. Antibacterial activity of ATP synthase inhibitors. Strains of AB and PA (labeled with ATCC strain number) were grown in liquid broth in the presence of 2–128 μg/mL inhibitor to determine MIC. Strains with known MDR profiles are labeled.

Compound	MIC (μg/mL)[a]		
	AB 17978	AB 1605 (MDR)	PA 2108 (MDR)
WSA236	64	64	32
WSA238	32	32	32
WSA248	>128	>128	>128
WSA249	32	64	16
WSA250	64	128	64
WSA251	128	>128	128
WSA252	64	64	64
WSA253	128	>128	128
WSA254	16	16	32
WSA255	16	16	32
WSA256	>128	>128	>128
WSA257	8	16	16
WSA261	8	16	64
WSA262	32	32	64
WSA269	>128	>128	>128
WSA270	16	16	32
Chloramphenicol	64	64	64

[a] MIC = minimum inhibitory concentration, defined as no visible growth and a >80% reduction in pathogen growth with compound compared to pathogen alone (DMSO only) as measured by OD 590 nm.

ChemMedChem

Research Article
doi.org/10.1002/cmdc.202400952

Chemistry Europe
European Chemical
Societies Publishing

As stated, in order for ATP synthase inhibitors to be effective antibiotics against Gram-negative bacteria like AB, PA, and EC, compounds must diffuse through the negatively charged, lipopolysaccharide outer membrane (OM), through the aqueous periplasm, and then embed in the *c* subunit of ATP synthase in the hydrophobic inner membrane (IM). For PA we found that the presence of a basic amine (NH$^+$ pK_a > 5) promotes OM diffusion,[19] which was supported by other recent work in the field.[20] Examination of the antibiotic activity of our C2 series of inhibitors (**WSA236**, **WSA238**, **WSA249**, **WSA248**, **WSA249**, and **WSA250**) indicated that presence of a basic amine also promotes activity against AB which has a similar but not identical OM to PA.[6] Larger basic amines, like benzyl pyrrolidine **WSA249**, were the most potent of the C2 series against MDRPA, and equipotent to piperidines **WSA236** and **WSA238** against both AB strains. Conversely, N-phenylpiperidine **WSA248**, (NH$^+$ pK_a ≈ 5) was inactive against both PA and AB.

Antibacterial activity against AB and PA of the western modifications did not directly correlate with ATP synthase inhibition in AB or PA (Figure 4) indicating that these modifications may also impact membrane diffusion/accumulation in the cell. Addition of the trimethoxy substituents at C6-C8 decreased antibacterial activity against both AB and PA for all C2 amines evaluated compared to the unmodified quinoline core with the same eastern substituents. For example, **WSA251** was 2- to 4-fold less potent than **WSA236** against AB and PA respectively.

Addition of the bromine at the C6 position increased activity against both susceptible and MDR AB strains for all C2 amines except the benzyl pyrrolidine series compared to the unmodi-

fied derivatives. However, against MDR PA the bromine either had no effect on two of the series (**WSA254** and **WSA255**), increased activity for the C2 N-methyl piperazine (**WSA257**) and decreased activity for C2 benzyl pyrrolidine (**WSA256**). Finally, addition of the phenyl group at C6 resulted (**WSA261**) in the most potent activity of the C2 N-ethyl piperidine series against both strains of AB, but diminished activity against MDR PA (**WSA261**). The C6 phenyl was similar in potency to the C6 bromine for the N-methyl piperazine series (**WSA270**) for both AB and PA. However, addition of the C6 phenyl to the other two C2 amines resulted in loss of activity against both bacteria. Taken together these findings indicate that there is a molecular size limitation, with larger analogs (like **WSA262**, **WSA256**, and **WSA269**) having reduced activity against both AB and PA, but that steric bulk is tolerated on both the western (**WSA270**) and eastern sides (**WSA249**) of the quinoline core, but not both (**WSA256** and **WSA269**). Additionally, significant differences between IC$_{50}$ values against AB and PA ATP synthase (Figure 3A) and potency trends (Figure 4) indicate that, despite the near sequence identity within the likely binding site (Figure 1D), inhibitors can be designed to have selective activity against ATP synthases from different species, even closely related ones.

Computational Docking

Demmer *et al.*[16] determined the cryo-EM structure of AB ATP synthase to 3.7 Å, which is sufficient to approximate the locations of side chains in the putative binding site for quinoline inhibitors. Therefore, we used Molecular Operating Environment (MOE; Chem Comp) software to predict possible binding poses for the synthesized inhibitors. Based on the cryo-EM structure of BDQ-bound MT ATP synthase, multiple binding sites for quinoline inhibitors are possible.[15] We opted to use the "leading" BDQ binding site, which lies on the edge of the subunit *a-c* interface. This site is centered at the proton-binding Asp60 residue on subunit *c* and includes aromatic side chains (Trp261 and Phe254) from subunit *a*, making it likely the highest affinity site. Additionally, we have shown previously that mutagenesis of *c*Ile65 in PA ATP synthase altered the IC$_{50}$ values of quinoline inhibitors, further supporting this site as the quinoline binding site.[18] During docking, the membrane bound location of the site was approximated by setting the external dielectric constant to 2. Representative high-scoring docking poses for several compounds are shown in Figure 5.

The experimental trends observed for inhibition of AB ATP synthase by these compounds (Figure 4) suggest that larger C2 amines generally increased potency. The addition of steric bulk to the western side of quinoline with a larger C2 substituent was detrimental, whereas the potency of a smaller C2 substituents could be improved by western modifications. Computational docking results (Figure 5) provide a visual representation of how the series of C2 amines and western modifications may affect binding, though docking scores did not correlate with *in vitro* activity. Interestingly, the binding pose of **WSA236** (Figure 5A) resembled the interactions observed for BDQ binding to MT ATP synthase, where the

Series	Compound	R^1	R^2	R^3	AB ATPS IC$_{50}$	PA ATPS IC$_{50}$	AB 17978 MIC	AB 1605 MIC	PA 2108 MIC
	WSA236	H	H	H	0.36	0.52	64	64	32
	WSA251	OMe	OMe	OMe	▲	▲	▲	▲	▲
	WSA254	Br	H	H	▽	▽	▽	▽	■
	WSA261	Ph	H	H	■	▲	▽	▽	▲
	WSA238	H	H	H	0.22	0.45	32	32	32
	WSA252	OMe	OMe	OMe	▲	▲	▲	▲	▲
	WSA255	Br	H	H	■	▽	▽	▽	■
	WSA262	Ph	H	H	▲	▲	■	■	▲
	WSA249	H	H	H	0.31	0.68	32	64	16
	WSA256	Br	H	H	■	▽	▲	▲	▲
	WSA269	Ph	H	H	■	■	▲	▲	▲
	WSA250	H	H	H	1.9	1.2	64	128	64
	WSA253	OMe	OMe	OMe	▽	▲	▲	▲	▲
	WSA257	Br	H	H	▽	▽	▽	▽	▽
	WSA270	Ph	H	H	▽	■	▽	▽	▽

Figure 4. Trends across western changes compared to unmodified within each C2. IC$_{50}$ or MIC for each unmodified quinoline (R^1-R^3 = H) are listed in μg/mL. For each modification, a *red arrow* indicates less potent activity (higher IC$_{50}$ or MIC), a *green arrow* indicates more potent activity (lower IC$_{50}$ or MIC), and a *black bar* indicates no change.

ChemMedChem

Research Article
doi.org/10.1002/cmdc.202400952

Chemistry
Europe

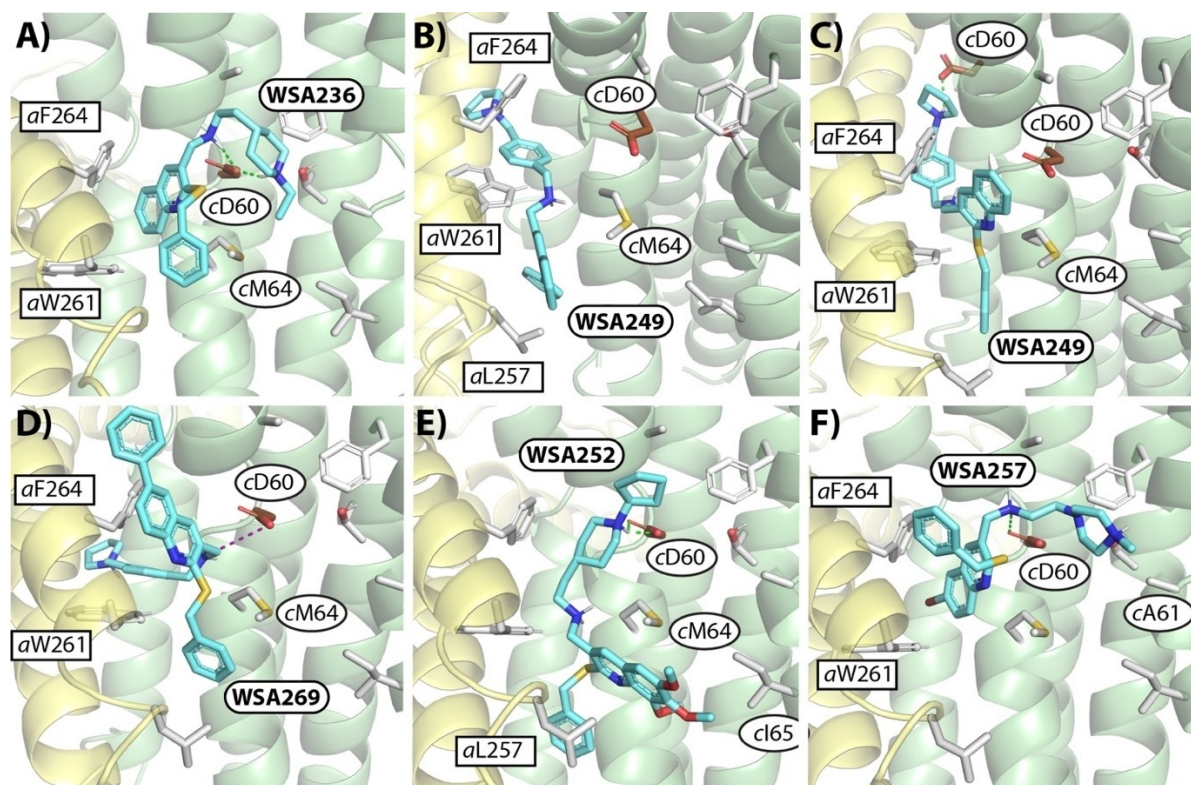European Chemical
Societies Publishing

Figure 5. Representative high-scoring docking poses, calculated in MOE and depicted using PyMol, are shown in the putative binding site (PDB ID: 7P2Y) at the interface of subunit *a* (pale yellow) and subunit *c* (pale green). Inhibitors WSA236 (A), WSA249 (B–C), WSA269 (D), WSA252 (E), and WSA257 (F) are shown in cyan. Specific interactions determined by MOE are shown as dashed lines with hydrogen bonds colored green and ionic interactions colored purple.

quinoline is inserted into the *a-c* interface, nitrogen on the C2 amine interacts with *c*Asp60, and the C1 S-benzyl group makes surface contacts with the binding site (see Figure S6). All four of the C2 amines formed hydrogen bonding or ionic interactions with Asp60 in most cases, though there were some exceptions, including the ability of benzyl pyrrolidine to reach deep into the *a-c* interface (Figure 5B) and even to interact with the adjacent Asp60 (Figure 5C). Western modifications tended to alter the position of the quinoline, excluding it from the *a-c* interface. This exclusion was most pronounced with phenyl and trimethoxy substituents (*e.g.* Figure 5, B–E), though the Br substituent was accommodated in some cases (*e.g.* **WSA257**, Figure 5F).

Conclusions

In summary, we have synthesized and evaluated 14 quinoline derivatives to explore if AB ATP synthase can be inhibited in an analogous fashion to our previous work developing PA ATP synthase inhibitors. In this series, we functionalized both the western (C6-C8) and eastern sides (C2) of the quinoline core and found that we can gain selectivity in AB versus PA ATP synthase via modification of the western side as demonstrated by C2 *N*-methyl piperazines **WSA250** (unmodified C6-C8, more active against PA ATP synthase), **WSA253** (C6-C8 trimethoxy, more active against AB ATP synthase), **WSA257** (C6 bromine,

equally active against both AB and PA ATP synthase), and **WSA270** (C6 phenyl, more active against AB ATP synthase). Functionalization of the western side of the quinoline also can increase inhibitory activity of less bulky C2 derivatives (**WSA250** *vs.* **WSA270**) for AB but not against PA; however, there is a size limit as demonstrated by the reduced activity of the largest analogs (**WSA262** and **WSA269**) against both AB and PA. None of the analogs selectively inhibited the electron transport chain of either bacterium; however, **WSA254**, **WSA255**, and **WSA257** were able to inhibit PA ETC in the low μg/mL range indicating that this could be a secondary target for future development. Finally, evaluation of the Hill Slope for this series indicated that for AB there is a second binding site that is engaged for some of the analogs, which is not as relevant in PA ATP synthase inhibition.

Each analog was also evaluated for antibacterial activity against susceptible strains for AB, SA, and EC as well as MDR clinical isolates of AB and PA. The most potent analogs overall against AB, with MICs between 8–16 ug/mL against one or both strains tested, were **WSA254**, **WSA255**, **WSA257**, **WSA261**, and **WSA270**. **WSA249** and **WSA257** were the most potent against the MDR PA strain. Molecular size directly impacted antibacterial activity against both PA and AB with the larger analogs like C2 benzyl pyrrolidines **WSA256** and **WSA269** and the C6-C8 trimethoxy series being the least potent. This work also demonstrated that the recently established OM penetration rules for PA[19,20] also promote OM penetration in AB.

Based on the findings described here, ATP synthase is a viable target for further antibiotic development in AB. Additionally, compounds show similar trends in *in vitro* activity and antibacterial activity in AB as observed in PA with some idiosyncrasies that could be further exploited to increase species specific selectivity.

Experimental

Synthesis and Spectroscopic Data

General. Reagents and solvents were purchased reagent-grade and used without further purification. All reactions were performed in flame-dried glassware under an Ar or N_2 atmosphere. Evaporation and concentration *in vacuo* was performed at 40–45 °C. TLC was conducted using precoated SiO_2 60 F254 glass plates from EMD with visualization by UV light (254 or 366 nm). NMR (^{1}H or ^{13}C) were recorded on an Varian INOVA-400 MHz spectrometer or a Bruker Avance-400 MHz spectrometer at 298 K. Residual solvent peaks were used as an internal reference ($CDCl_3$ with 0.1 % TMS). Coupling constants (*J*) (H,H) are given in Hz. Coupling patterns are designated as singlet (s), doublet (d), triplet (t), multiplet (m) or quartet (q). Low-resolution mass spectral data were acquired on a Shimadzu single quadrupole LCMS-2020. High-resolution mass spectral Samples were analyzed with a Q Exactive HF−X (Thermo-Fisher, Bremen, Germany) mass spectrometer. Samples were introduced via a heated electrospray source (HESI) at a flow rate of 10 µL/min. HESI source conditions were set as: nebulizer temperature 400 °C, sheath gas (nitrogen) 20 arb, auxiliary gas (nitrogen) 0 arb, sweep gas (nitrogen) 0 arb, capillary temperature 320 degrees C, RF voltage 45 V. The mass range was set to 100–1000 m/z. All measurements were recorded at a resolution setting of 120,000. Solutions were analyzed at 0.1 mg/mL or less based on responsiveness to the ESI mechanism. Xcalibur (ThermoFisher, Breman, Germany) was used to analyze the data. Molecular formula assignments were determined with Molecular Formula Calculator (v 1.3.0). All observed species were singly charged, as verified by unit *m/z* separation between mass spectral peaks corresponding to the ^{12}C and ^{13}C^{12}C$_{c-1}$ isotope for each elemental composition.

General Procedure 1: Nucleophilic Aromatic Substitution. The chloroquinoline carbaldehyde (1 eq) and Na_2S (1.6 eq) were dissolved in *N,N*-dimethylformamide (0.2 M) and allowed to stir at 23 °C for 15 hours. Then K_2CO_3 (1.5 eq) and benzyl bromide (1.5 eq) were added, and the solution was warmed to 100 °C for 2 hours. After 2 hours, the reaction was cooled to 23 °C and diluted with DI H_2O. The solution was then extracted with ethyl acetate (3x). The organic layers were then combined and concentrated under reduced pressure. Flash chromatography of the crude extracts (SiO_2, 5×15 cm, 0–10 % ethyl acetate/hexanes gradient elution) provided the desired product.

General Procedure 2: Reductive Amination. The benzyl sulfide quinoline (1 eq) and amine (1.2 eq) were dissolved in anhydrous methanol (0.09 M) under inert conditions. *N,N*-Diisopropylethylamine (3 eq) was then added dropwise, and the reaction was allowed to stir at 23 °C for 24 h. $NaBH_4$ (2 eq) was then added. After 1 h, the reaction was diluted with DI H_2O and extracted with dichloromethane (2x) or ethyl acetate (3x). The organic layers were then combined, dried over Na_2SO_4, and concentrated under reduced pressure. Flash chromatography of the crude extracts (SiO_2, 3×10 cm, 0–100 % CH_3OH/CH_2Cl_2 gradient elution) provided the desired products.

General Procedure 3: Suzuki Coupling Reactions. To a flame dried reaction flask were sequentially added brominated quinoline intermediate (1 equiv.), (ii) Cs_2CO_3 (2 equiv.), (iii) boronic acid derivative (1.5 equiv.), (iv) $Pd(PPh_3)_4$ (0.2 equiv.), as well as (v) toluene (0.1 M). The reaction solution was sparged with argon and then heated to 90 °C for 16 hours. The solution was cooled to room temperature, filtered through a pad of Celite, and rinsed with DCM. Purification of the solution was carried out via TLC in 10 % CH_3OH/CH_2Cl_2 or flash chromatography of the crude extracts (SiO_2, 3×10 cm, 0–100 % CH_3OH/CH_2Cl_2 gradient elution) providing the desired product.

2-(benzylthio)-6,7,8-trimethoxyquinoline-3-carbaldehyde (**5**). 2-chloro-6,7,8-trimethoxyquinoline-3-carbaldehyde (**2**, 500 mg, 1.77 mmol), sodium sulfide (221 mg, 2.84 mmol), and benzyl bromide (0.32 mL, 2.66 mmol) were reacted using general procedure **1** to produce 2-(benzylthio)-6,7,8-trimethoxyquinoline-3-carbaldehyde (**5**, 382 mg, 58 % yield) as a yellow solid. ^{1}H NMR (400 MHz, $CDCl_3$) δ 10.20 (s, 1H), 8.64 (s, 1H), 7.47 (d, *J* = 7.2 Hz, 2H), 7.31-7.20 (m, 3H), 7.13 (s, 1H), 4.61 (s, 2H), 4.11 (s, 3H), 4.05 (s, 3H), 3.96 (s, 3H). ^{13}C NMR ($CDCl_3$, 100 MHz): δ 189.93, 159.50, 158.77, 148.39, 147.59, 140.05, 138.05, 137.67, 129.48, 128.56, 127.19, 125.20, 115.77, 103.13, 61.86, 61.49, 56.49, 34.14. HRMS (ESI) *m/z* [M + H]$^+$ calcd for $C_{20}H_{20}NO_4S$ 370.1108; found 370.11028.

2-(benzylthio)-6-bromoquinoline-3-carbaldehyde (**6**). 6-bromo-2-chloroquinoline-3-carbaldehyde (**3**, 500 mg, 1.85 mmol) sodium sulfide (346 mg, 4.44 mmol) and benzyl bromide (.328 mL, 2.77 mmol) were reacted using general procedure **1** to produce intermediate **6** (310 mg, 47 %) as a yellow solid. ^{1}H NMR (400 MHz, $CDCl_3$) δ 10.26 (s, 1H), 8.31 (s, 1H), 7.97 (d, *J* = 1.5 Hz, 1H), 7.85 (t, *J* = 2.3 Hz, 2H), 7.49 (d, *J* = 7.2 Hz, 2H), 7.30 (t, *J* = 7.3 Hz, 2H), 7.23 (t, *J* = 8.3 Hz, 1H), 4.62 (s, 2H). ^{13}C NMR (100 MHz, $CDCl_3$) δ189.52, 159.38, 147.98, 141.07, 137.55, 136.26, 131.03, 129.69, 129.44, 128.50, 127.58, 127.25, 125.82, 119.75, 34.17. HRMS (ESI) *m/z* [M + H]$^+$ calcd for $C_{17}H_{13}BrNOS$ 357.9896; found 357.98935.

1-(2-(benzylthio)quinolin-3-yl)-N-(4-(piperidin-1-yl)benzyl)methanamine (**WSA248**). 2-(benzylthio)quinoline-3-carbaldehyde (**4**, 200 mg, 0.72 mmol) and (4-(piperidin-1-yl)phenyl)methanamine (0.31 mL, 0.86 mmol) were reacted using general procedure **2** to produce compound **WSA248** (103 mg, 32 %) as a red semi solid. ^{1}H NMR (400 MHz, $CDCl_3$) δ 7.98 (d, *J* = 8.4 Hz, 1H), 7.92 (s, 1H), 7.70 (d, *J* = 8.0 Hz, 1H), 7.61 (m, *J* = 4.1 Hz, 1H), 7.48 (d, *J* = 7.3 Hz, 2H), 7.40 (t, *J* = 7.50 Hz, 1H), 7.28 (t, *J* = 7.4 Hz, 2H), 7.21 (t, *J* = 7.0 Hz, 3H), 6.89 (d, *J* = 8.6 Hz, 2H), 4.65 (s, 2H), 3.88 (s, 2H), 3.72 (s, 2H), 3.11 (t, *J* = 5.4 Hz, 4H), 1.69 (m, 4H), 1.55 (q, *J* = 5.7 Hz, 2H). ^{13}C NMR (100 MHz, $CDCl_3$) δ 158.31, 151.49, 147.06, 138.44, 133.86, 131.29, 130.51, 129.40, 129.16, 129.11, 128.52, 127.69, 127.53, 127.12, 126.14, 125.35, 116.63, 52.83, 50.87, 49.33, 34.06, 25.93, 24.36. HRMS (ESI) *m/z* [M + H]$^+$ calcd for $C_{29}H_{32}N_3S$ 454.2311; found 454.23071.

1-(2-(benzylthio)quinolin-3-yl)-N-(4-(pyrrolidin-1-ylmethyl)benzyl)methanamine (**WSA249**). 2-(benzylthio)quinoline-3-carbaldehyde (**4**, 200 mg, 0.72 mmol) and (4-(pyrrolidin-1-ylmethyl)phenyl)methanamine (0.15 mL, 0.86 mmol) were reacted using General procedure **2** to produce compound **WSA249** (211 mg, 65 %) as a brown semi solid. ^{1}H NMR (400 MHz, $CDCl_3$) δ 7.98 (d, *J* = 8.3 Hz, 1H), 7.92 (s, 1H), 7.70 (d, *J* = 8.1 Hz, 1H), 7.62 (t, *J* = 8.3 Hz, 2H), 7.45 (d, *J* = 16.4 Hz, 1H), 7.39 (t, *J* = 7.2 Hz, 1H), 7.33-7.19 (m, 7H), 4.65 (s, 2H), 3.88 (s, 2H), 3.79 (s, 2H), 3.67 (s, 12H), 2.60 (s, 4H), 1.80 (m, 4H). ^{13}C NMR (100 MHz, $CDCl_3$) δ 158.24, 147.07, 139.19, 138.40, 136.40, 133.93, 131.12, 129.42, 129.37, 129.22, 128.52, 128.33, 127.68, 127.51, 127.13, 126.08, 125.40, 60.02, 53.94, 53.02, 49.50, 34.06, 23.38. HRMS (ESI) *m/z* [M + H]$^+$ calcd for $C_{29}H_{32}N_3S$ 454.2311; found 454.23093.

ChemMedChem

Research Article
doi.org/10.1002/cmdc.202400952

**Chemistry
Europe**

European Chemical
Societies Publishing

N-((2-(benzylthio)quinolin-3-yl)methyl)-2-(4-methylpiperazin-1-yl)ethan-1-amine (WSA250). 2-(benzylthio)quinoline-3-carbaldehyde (**4**, 300 mg, 1.07 mmol) and 2-(4-methylpiperazin-1-yl)ethan-1-amine (0.20 mL, 1.29 mmol) were reacted using general procedure **2** to produce compound **WSA250** (133 mg, 30%) as a yellow semi solid. ^{1}H NMR (400 MHz, CDCl$_3$) δ 7.98 (t, $J = 7.9$ Hz, 2H), 7.73 (d, $J = 7.9$ Hz, 1H), 7.64 (t, $J = 7.4$ Hz, 1H), 7.49 (d, $J = 7.2$ Hz, 2H), 7.43 (t, $J = 7.1$ Hz, 1H), 7.30 (t, $J = 7.3$ Hz, 2H), 7.23 (t, $J = 7.4$ Hz, 1H), 4.67 (s, 2H), 3.92 (s, 2H), 2.75 (t, $J = 5.9$ Hz, 2H), 2.55 (t, $J = 5.9$ Hz, 2H), 2.50 (s, 7H), 2.30 (s, 3H). ^{13}C NMR (100 MHz, CDCl$_3$) δ 158.10, 147.11, 138.28, 134.36, 130.56, 129.35, 128.53, 127.65, 127.51, 127.17, 126.04, 125.46, 57.07, 54.71, 52.41, 50.13, 45.58, 45.51, 33.99. HRMS (ESI) m/z [M+H]$^+$ calcd for C$_{24}$H$_{31}$N$_4$S 407.2264; found 407.22600.

N-((2-(benzylthio)-6,7,8-trimethoxyquinolin-3-yl)methyl)-2-(1-ethylpiperidin-4-yl)ethan-1-amine (WSA251). 2-(benzylthio)-6,7,8-trimethoxyquinoline-3-carbaldehyde (**5**, 50 mg, 0.135 mmol) and 2-(1-ethylpiperidin-4-yl)ethan-1-amine (28 uL, 0.16 mmol) were reacted using general procedure **2** to produce **WSA251** (42 mg, 61% yield) as a dark yellow semi-solid. ^{1}H NMR (400 MHz, CDCl$_3$) δ 8.09 (s, 1H), 7.46 dt, $J = 8.0$ Hz, 2H), 7.29 (t, $J = 6.8$ Hz, 2H), 7.24 (d, $J = 7.1$ Hz, 1H), 7.15 (s, 1H), 4.64 (s, 2H), 4.05 (s, 3H), 4.02 (s, 3H), 3.96 (s, 3H), 3.88 (s, 2H), 2.98 (d, $J = 11.3$ Hz, 2H), 2.66 (t, $J = 7.1$ Hz, 2H), 2.46 (q, $J = 7.2$ Hz, 2H), 1.94 (t, $J = 10.9$ Hz, 2H), 1.69 (d, $J = 10.2$ Hz, 2H), 1.47 (q, $J = 6.4$ Hz, 2H), 1.40-1.30 (m, 3H), 1.13 (t, $J = 7.2$ Hz, 3H). ^{13}C NMR (CDCl$_3$, 100 MHz): δ 157.78, 155.87, 147.37, 145.00, 140.10, 138.57, 129.37, 129.02, 128.63 (2 C), 127.22, 116.65, 103.20, 61.74, 61.39, 56.22, 53.40, 52.69, 50.86, 46.79, 36.68, 34.27, 33.55, 31.90, 11.80. HRMS (ESI) m/z [M+H]$^+$ calcd for C$_{29}$H$_{40}$N$_3$O$_3$S 510.2785; found 510.27827.

N-((2-(benzylthio)-6,7,8-trimethoxyquinolin-3-yl)methyl)-2-(1-cyclopentylpiperidin-4-yl)ethan-1-amine (WSA252). 2-(benzylthio)-6,7,8-trimethoxyquinoline-3-carbaldehyde (**5**, 50 mg, 0.135 mmol) and 2-(1-cyclopentylpiperidin-4-yl)ethan-1-amine (33 uL, 0.16 mmol) were reacted using general procedure **2** to produce **WSA252** (45 mg, 60% yield) as a yellow semi-solid. ^{1}H NMR (400 MHz, CDCl$_3$) δ 8.08 (s, 1H), 7.45 (d, $J = 7.2$ Hz, 2H), 7.30 (t, $J = 7.3$ Hz, 2H), 7.24 (d, $J = 7.2$ Hz, 1H), 7.15 (s, 1H), 4.63 (s, 2H), 4.05 (s, 3H), 4.01 (s, 3H), 3.96 (s, 3H), 3.87 (s, 2H), 3.13 (d, $J = 10.5$ Hz, 2H), 2.65 (t, $J = 6.7$ Hz, 3H), 2.04 (m, 2H), 1.89 (m, 2H), 1.72-1.44 (m, 14H). ^{13}C NMR (CDCl$_3$, 100 MHz): δ 157.80, 155.90, 147.37, 145.02, 140.11, 138.58, 129.38, 129.07, 128.99, 128.64, 127.22, 16.65, 103.21, 67.99, 61.75, 61.39, 56.23, 52.75, 50.88, 46.66, 36.36, 34.30, 33.18, 31.40, 29.95, 24.22. HRMS (ESI) m/z [M+H]$^+$ calcd for C$_{32}$H$_{44}$N$_3$O$_3$S 550.3098; found 550.30958.

N-((2-(benzylthio)-6,7,8-trimethoxyquinolin-3-yl)methyl)-2-(4-methylpiperazin-1-yl)ethan-1-amine (WSA253). 2-(benzylthio)-6,7,8-trimethoxyquinoline-3-carbaldehyde (**5**, 50 mg, 0.135 mmol) and 2-(4-methylpiperazin-1-yl)ethan-1-amine (25 uL, 0.16 mmol) were reacted using general procedure **2** to produce **WSA253** (31 mg, 46% yield) as a orange semi-solid. ^{1}H NMR (400 MHz, CDCl$_3$) δ 8.11 (s, 1H), 7.46 (d, $J = 7.2$ Hz, 2H), 7.32-7.24 (m, 3H), 7.15 (s, 1H), 4.64 (s, 2H), 4.05 (s, 3H), 4.02 (s, 3H), 3.96 (s, 3H), 3.91 (s, 1H), 2.73 (t, $J = 6.0$ Hz, 2H), 2.53 (t, $J = 6.0$ Hz, 2H), 2.54-2.43 (m, 8H), 2.27 (s, 3H). ^{13}C NMR (CDCl$_3$, 100 MHz): δ 157.79, 155.95, 147.43, 145.08, 140.13, 138.54, 129.41, 129.30, 128.68 (2 C), 127.27, 116.69, 103.22, 61.78, 61.41, 57.58, 56.25, 55.16, 53.03, 50.78, 46.05, 45.81, 34.25. HRMS (ESI) m/z [M+H]$^+$ calcd for C$_{27}$H$_{37}$N$_4$O$_3$S 497.2581; found 497.25777.

N-((2-(benzylthio)-6-bromoquinolin-3-yl)methyl)-2-(1-ethylpiperidin-4-yl)ethan-1-amine (WSA 254). 2-(benzylthio)-6-bromoquinoline-3-carbaldehyde (**6**, 600 mg, 1.67 mmol) and 2-(1-ethylpiperidin-4-yl)ethan-1-amine (0.35 mL, 2.00 mmol) were reacted using general procedure **2** to produce **WSA254** (289 mg, 35%) as an orange semi solid. ^{1}H NMR (400 MHz, CDCl$_3$) δ 7.85 (m, $J = 5.4$ Hz, 3H), 7.70 (q, $J = 3.7$ Hz, 1H), 7.47 (d, $J = 7.2$ Hz, 2H), 7.31 (t, $J = 7.3$ Hz, 2H), 7.25

(t, $J = 9.3$ Hz, 1H), 4.63 (s, 2H), 3.87 (s, 2H), 3.09 (d, $J = 11.2$ Hz, 2H), 2.66 (t, $J = 6.8$ Hz, 2H), 2.57 (q, $J = 7.2$ Hz, 2H), 2.06 (t, $J = 10.7$ Hz, 2H), 1.72 (d, $J = 10.0$ Hz, 2H), 1.49 (t, $J = 6.1$ Hz, 5H), 1.20 (t, $J = 7.2$ Hz, 3H). ^{13}C NMR 100 MHz CDCl$_3$ δ 159.01, 145.60, 138.01, 132.68, 132.52, 132.22, 129.44, 129.38, 129.33, 128.54, 127.22, 118.81, 52.95, 52.43, 50.19, 46.66, 36.23, 34.15, 33.03, 31.03, 11.14 HRMS (ESI) m/z [M+H]$^+$ calcd for C$_{26}$H$_{33}$BrN$_3$S 498.1573; found 498.15686.

N-((2-(benzylthio)-6-bromoquinolin-3-yl)methyl)-2-(1-cyclopentylpiperidin-4-yl)ethan-1-amine (WSA255). 2-(benzylthio)-6-bromoquinoline-3-carbaldehyde (**6**, 549 mg, 1.54 mmol) and 2-(1-cyclopentylpiperidin-4-yl)ethan-1-amine (0.45 mL, 1.69 mmol) were reacted using general procedure **2** to produce **WSA255** (308 mg, 37%) as a yellow semi solid. ^{1}H NMR (400 MHz, CDCl$_3$) δ 7.82 (m, $J = 4.6$ Hz, 3H), 7.67 (dd, $J = 2.2, 8.9$ Hz, 1H), 7.47 (d, $J = 7.1$ Hz, 2H), 7.29 (t, $J = 7.3$ Hz, 2H), 7.23 (t, $J = 7.2$ Hz, 1H), 4.62 (s, 2H), 3.84 (s, 2H), 3.00 (d, $J = 11.6$ Hz, 2H), 2.65 (t, $J = 7.3$ Hz, 2H), 2.43 (m, $J = 8.1$ Hz, 1H), 1.86 (d, $J = 10.8$ Hz, 4H), 1.66 (t, $J = 10.8$ Hz, 4H), 1.52 (m, $J = 4.1$ Hz, 2H), 1.45 (d, $J = 14.4$ Hz, 4H), 1.30 (t, $J = 10.7$ Hz, 3H). ^{13}C NMR (100 MHz, CDCl$_3$) δ 158.94, 145.54, 137.98, 132.46, 132.42, 132.35, 129.43, 129.36, 129.31, 128.52, 127.24, 127.20, 118.74, 77.47, 77.15, 76.84, 67.76, 52.85, 50.07, 46.93, 36.7847, 34.12, 33.58, 32.20, 30.55, 24.21. HRMS (ESI) m/z [M+H]$^+$ calcd for C$_{29}$H$_{37}$BrN$_3$S 538.1886; found 538.18858.

1-(2-(benzylthio)-6-bromoquinolin-3-yl)-N-(4-(pyrrolidin-1-ylmethyl)benzyl)methanamine (WSA256). 2-(benzylthio)-6-bromoquinoline-3-carbaldehyde (**6**, 500 mg, 1.39 mmol) and (4-(pyrrolidin-1-ylmethyl)phenyl)methanamine (0.25 mL, 1.39 mmol) were reacted using general procedure **2** to produce **WSA256** (310 mg, 42%) as a dark orange semi solid. ^{1}H NMR (400 MHz, CDCl$_3$) δ 7.82 (d, $J = 1.8$ Hz, 1H), 7.80 (t, $J = 2.0$ Hz, 2H), 7.65 (dd, $J = 2.1, 9.0$ Hz, 1H), 7.46 (d, $J = 7.2$ Hz, 2H), 7.29 (q, $J = 6.8$ Hz, 6H), 7.21 (t, $J = 7.1$ Hz, 1H), 4.60 (s, 2H), 3.85 (s, 2H), 3.78 (s, 2H), 3.61 (s, 2H), 2.52 (s, 4H), 1.78 (s, 4H). ^{13}C NMR (100 MHz, CDCl$_3$) δ 158.98, 145.54, 138.68, 138.06, 137.60, 132.51, 132.44, 132.26, 129.48, 129.38, 129.36, 129.24, 128.55, 128.18, 127.24, 127.22, 118.75, 77.51, 77.19, 76.87, 60.31, 54.11, 53.11, 49.23, 34.13, 23.44. HRMS (ESI) m/z [M+H]$^+$ calcd for C$_{29}$H$_{31}$BrN$_3$S 532.1417; found 532.14163.

N-((2-(benzylthio)-6-bromoquinolin-3-yl)methyl)-2-(4-methylpiperazin-1-yl)ethan-1-amine (WSA257) 2-(benzylthio)-6-bromoquinoline-3-carbaldehyde (**6**, 415 mg, 1.15 mmol) and 2-(4-methylpiperazin-1-yl)ethan-1-amine (213 uL, 1.39 mmol) were reacted using general procedure **2** to produce **WSA257** (276 mg, 49% yield) as an orange semi-solid. ^{1}H NMR (400 MHz, CDCl$_3$) δ 7.86-7.82 (m, 3H), 7.68 (dd, $J = 8.8, 2$ Hz, 1H), 7.48 (d, $J = 7.2$ Hz, 2H), 7.30 (t, $J = 7.3$ Hz, 2H), 7.26-7.23 (m, 1H), 4.63 (s, 2H), 3.88 (s, 2H), 2.73 (t, $J = 6.0$ Hz, 2H), 2.52 (t, $J = 5.9$ Hz, 2H), 2.70-2.15 (m, 8H), 2.29 (s, 3H). ^{13}C NMR (CDCl$_3$, 100 MHz): δ 158.98, 145.57, 137.97, 132.51, 132.43, 132.31, 129.44, 129.37, 129.34, 128.54, 127.28, 127.22, 118.73, 57.57, 55.14, 53.16, 50.04, 46.11, 45.92, 34.09. HRMS (ESI) m/z [M+H]$^+$ calcd for C$_{24}$H$_{30}$BrN$_4$S 485.1369; found 485.13664.

N-((2-(benzylthio)-6-phenylquinolin-3-yl)methyl)-2-(1-ethylpiperidin-4-yl)ethan-1-amine (WSA261). N-((2-(benzylthio)-6-bromoquinolin-3-yl)methyl)-2-(1-ethylpiperidin-4-yl)ethan-1-amine (**7**, 100 mg, 0.20 mmol) and phenyl boronic acid (37 mg, 0.30 mmol) were reacted using general procedure **3** to produce **WSA261** (62 mg, 62%) as a yellow semi-solid. ^{1}H NMR (400 MHz, CDCl$_3$) δ 8.05 (d, $J = 8.4$ Hz, 1H), 7.92 (m, $J = 8.4$ Hz, 3H), 7.70 (t, $J = 4.2$ Hz, 2H), 7.49 (m, $J = 4.3$ Hz, 4H), 7.38 (t, $J = 7.4$ Hz, 1H), 7.31 (t, $J = 7.3$ Hz, 2H), 7.24 (t, $J = 7.6$ Hz, 1H), 4.68 (s, 2H), 3.89 (s, 2H), 2.98 (d, $J = 11.4$ Hz, 2H), 2.67 (t, $J = 7.2$ Hz, 2H), 2.45 (q, $J = 7.2$ Hz, 2H), 1.93 (t, $J = 10.9$ Hz, 2H), 1.69 (d, $J = 10.0$ Hz, 2H), 1.49 (q, $J = 6.6$ Hz, 2H), 1.38 (d, $J = 5.9$ Hz, 4H), 1.25 (s, 1H), 1.12 (t, $J = 7.2$ Hz, 3H). ^{13}C NMR (100 MHz, CDCL$_3$) δ 158.27, 146.46, 140.54, 138.33, 138.08, 134.07,

131.65, 129.36, 128.97, 128.81, 128.53, 128.08, 127.53, 127.34, 127.16, 126.26, 125.23, 53.28, 52.57, 50.37, 46.77, 36.60, 34.11, 33.45, 31.79, 29.75 HRMS (ESI) *m/z* [M+H]$^+$ calcd for $C_{32}H_{38}N_3S$ 496.2781; found 496.27778.

N-((2-(benzylthio)-6-phenylquinolin-3-yl)methyl)-2-(1-cyclopentyl-piperidin-4-yl)ethan-1-amine (WSA262). N-((2-(benzylthio)-6-bro-moquinolin-3-yl)methyl)-2-(1-cyclopentylpiperdin-4-yl)ethan-1-amine (**8**, 76 mg, 0.14 mmol) and phenylboronic acid (26 mg, 0.21 mmol) were reacted using general procedure **3** to produce **WSA262** (25 mg, 33%) as a light-yellow semi-solid. ^{1}H NMR (400 MHz, CDCl$_3$) δ 8.05 (d, J=8.3 Hz, 1H), 7.97 (s, 1H), 7.91 (d, J= 8.4 Hz, 2H), 7.71 (d, J=7.0 Hz, 2H), 7.49 (t, J=7.9 Hz, 4H), 7.39 (t, J= 7.4 Hz, 1H), 7.31 (t, J=7.3 Hz, 2H), 7.24 (t, J=7.5 Hz, 2H), 4.68 (s, 2H), 3.91 (s, 2H), 2.99 (d, J=11.7 Hz, 2H), 2.68 (t, J=7.3 Hz, 2H), 2.40 (m, J=8.2 Hz, 1H), 1.85 (t, J=10.7 Hz, 4H), 1.66 (m, J=9.5 Hz, 4H), 1.51 (m, J=5.5 Hz, 4H), 1.38 (m, J=7.6 Hz, 3H), 1.26 (m, J=6.6 Hz, 3H). ^{13}C NMR (100 MHz, CDCl$_3$) δ 158.24, 146.45, 140.57, 138.30, 138.06, 134.01, 131.69, 129.33, 128.95, 128.78, 128.51, 128.07, 127.50, 127.34, 127.13, 126.27, 125.23, 67.80, 52.94, 50.31, 46.88, 36.87, 34.08, 33.69, 32.40, 30.69, 24.23. HRMS (ESI) *m/z* [M+H]$^+$ calcd for $C_{35}H_{42}N_3S$ 536.3094; found 536.30932.

1-(2-(benzylthio)-6-phenylquinolin-3-yl)-N-(4-(pyrrolidin-1-ylmethyl)benzyl)methanamine (WSA269). 1-(2-(benzylthio)-6-bro-moquinoline-3-yl)-N-(4-(pyrrolidin-1-ylmethyl)benzyl)methanamine (**9**, 100 mg, 0.19 mmol) and phenylboronic acid (34 mg, 0.28 mmol) were reacted using general procedure **3** to produce **WSA269** (80 mg, 80%) as a yellow-orange semi-solid. ^{1}H NMR (400 MHz, CDCl$_3$) δ 8.05 (d, J=8.5 Hz, 1H), 7.99 (s, 1H), 7.91 (m, J=4.2 Hz, 2H), 7.70 (d, J=7.2 Hz, 2H), 7.49 (t, J=8.4 Hz, 4H), 7.41 (t, J=6.3 Hz, 2H), 7.36 (t, J=6.9 Hz, 2H), 7.30 (t, J=14.6 Hz, 2H), 7.23 (t, J=8.1 Hz, 1H), 4.67 (s, 2H), 3.91 (s, 2H), 3.86 (s, 2H), 3.82 (s, 2H), 2.83 (s, 4H), 1.92 (s, 4H). ^{13}C NMR (100 MHz, CDCl$_3$) δ 158.24, 146.47, 140.50, 140.26, 138.35, 138.08, 134.11, 131.45, 129.90, 129.35, 128.98, 128.83, 128.60, 128.52, 128.08, 127.54, 127.34, 127.15, 126.24, 125.26, 77.43, 77.12, 76.80, 59.24, 53.50, 52.87, 49.49, 34.08, 23.25. HRMS (ESI) *m/z* [M+H]$^+$ calcd for $C_{35}H_{36}N_3S$ 530.2624; found 530.26232.

N-((2-(benzylthio)-6-phenylquinolin-3-yl)methyl)-2-(4-methylpi-perazin-1-yl)ethan-1-amine (WSA270). N-((2-(benzylthio)-6-bromo-quinolin-3-yl)methyl)-2-(4-methylpiperazin-1-yl)ethan-1-amine (**10**, 20 mg, 0.04 mmol) and phenylboronic acid (7 mg, 0.06 mmol) were combined using general procedure **3** to produce **WSA270** (8.3 mg, 41% yield) as a pale yellow semi-solid. ^{1}H NMR (400 MHz, CDCl$_3$) δ 8.05 (d, J=8.5 Hz, 1H), 8.00 (s, 1H), 7.92 (m, J=3.0 Hz, 1H), 7.71 (t, J=4.2 Hz, 1H), 7.50 (m, J=3.8 Hz, 1H), 7.40 (d, J=7.4 Hz, 1H), 7.32 (d, J=7.1 Hz, 1H), 7.25 (s, 1H), 4.69 (s, 1H), 3.93 (s, 1H), 2.76 (t, J= 6.0 Hz, 1H), 2.54 (t, J=6.1 Hz, 1H), 2.42 (q, J=6.1 Hz, 1H), 2.26 (s, 1H). ^{13}C NMR (CDCl$_3$, 100 MHz): δ 158.24, 146.41, 140.53, 138.23, 138.00, 133.98, 131.55, 129.31, 128.91, 128.74, 128.47, 128.02, 127.46, 127.29, 127.10, 126.23, 125.19, 5754, 55.08, 53.09, 50.21, 46.04, 45.82, 34.00. HRMS (ESI) *m/z* [M+H]$^+$ calcd for $C_{30}H_{35}N_4S$ 483.2577; found 483.25738.

Biological Evaluation

General Sterilization Procedure. The following are general steps, unless otherwise noted. All steps were completed with aseptic techniques. All media and glassware were sterilized via autoclave at 121 °C for 60 minutes. All agitation occurred at 160 rpm in a temperature-controlled console shaker (Excella E25) at 37 °C. Full strength tryptic soy broth (TSB) was made by dissolving 30 g BD Bacto TSB powder in 1 L deionized water. All bacterial strains were purchased from ATCC (*Acinetobacter baumannii* (ATCC 17978 and ATCC 1605, MDR), *Pseudomonas aeruginosa* (BAA-2108, MDR),

Staphylococcus aureus (ATCC 29213), and *Escherichia coli* (ATCC 25922).

Antimicrobial Susceptibility Assay Procedure. Susceptibility testing was performed in biological triplicate, using the broth microdilution method as outlined by the Clinical and Laboratory Standards Institute. Briefly, minimum inhibitory concentrations (MIC) determi-nations were carried out in 96-well microtiter plates with 2-fold serial dilutions of the compounds from 0 μg/mL to 128 μg/mL (final assay concentrations) in DMSO. Briefly, to each well 1 μL of compound in DMSO, 89 μL of tryptic soy broth (TSB), and 10 μL of bacterial inoculum, grown from frozen stock in 10 mL of TSB for 4–6 hours, were added. After incubation for 12–15 h at 37 °C, absorbance at 590 nm was read on a Biotek Synergy HTX Multi-mode plate reader. Data was processed by background subtracting the media absorbance and then normalizing the data to full bacterial growth with only vehicle. MIC is defined as the lowest concentration of antibiotic that achieves ≥ 80% growth inhibition, which corresponds to no visible growth.

Preparation of Inverted Inner Membrane Vesicles. *Acinetobacter baumannii* (ATCC 17978) and *Pseudomonas aeruginosa* (ATCC 9027) cells were grown in LB medium at 37 °C with shaking at 150 rpm and harvested by centrifugation in the late exponential phase of growth. Cells were resuspended in TMG buffer (50 mM Tris-HCl, pH 7.5, 5 mM MgCl$_2$, 10% v/v glycerol) with 1 mM phenylmethane-sulfonyl fluoride, 1 mM dithiothreitol, and a small amount of DNase and lysed by two passes through an Avestin B15 homogenizer at 19,000 psi. Lysate was cleared by centrifugation at 9,000 x *g* and inverted membrane vesicles were collected from the supernatant by centrifugation at 169,000 x *g*. To reduce background ATP synthesis activity in AB vesicles, it was important to wash the membranes by resuspending in TMG buffer and centrifuging again at 169,000 x *g*. Washed pellets were resuspended in TMG buffer, and aliquots were stored at −80 °C. Once thawed, aliquots were not refrozen. Protein concentration in membrane vesicles was deter-mined using a modified Lowry assay.[26]

Determination of ATP synthesis activity. *In vitro* ATP synthesis activity of inverted membrane vesicles was measured as previously described.[18,19] A reaction solution was prepared containing 5 mM tricine-KOH, pH 8.0, 50 mM KCl, 2.5 mM MgCl$_2$, 0.1 mM adenosine diphosphate, 3.75 mM potassium phosphate, and 2.5 mM NADH and distributed into a 96-well plate. NADH-driven ATP synthesis was initiated by addition of inverted vesicles to 50 μg/mL and allowed to proceed for 10 min. The reaction was stopped by transferring an aliquot into 1% trichloroacetic acid. The stopped reaction was diluted 100 fold with deionized water and a sample was transferred to luciferase solution containing 25 mM Tricine-NaOH, pH 7.8, 5 mM MgSO$_4$, 0.1 mM EDTA, 0.1 mM NaN$_3$, 150 μg/mL luciferin, and 7.5 μg/mL luciferase. Luminescence was measured in an opaque white 96-well plate using a BioTek H1 multi-mode plate reader. Each replicate set included a positive control containing DMSO with no compound and a negative control containing carbonyl cyanide 3-chlorophenylhydrazone (CCCP). Luminescence values were corrected for background by subtracting the CCCP control and normalized to the luminescence of the DMSO control. Normalized activity was fit using a variable-slope dose response curve. Nonlinear regression, including prediction of 95% confidence bands, and pairwise comparisons of fits using the F-test method were completed using GraphPad Prism10.

Determination of ETC activity. NADH-driven proton pumping activity in inverted membrane vesicles was measured as previously described.[18] Briefly, vesicles were diluted to 0.5 mg/mL in HMK buffer (50 mM HEPES, 2 mM MgCl$_2$, 300 mM KCl, pH 7.5) with 0.3 μg/mL 9-amino-6-chloro-2-methoxyacridine (ACMA) and distrib-uted into wells of a black 96-well plate containing various

ChemMedChem

Research Article
doi.org/10.1002/cmdc.202400952

Chemistry Europe
European Chemical
Societies Publishing

concentrations of inhibitors dissolved in DMSO. ACMA fluorescence ($\lambda_{ex} = 415$ nm, $\lambda_{em} = 485$ nm) was monitored using a BioTek H1 multi-mode plate reader. Proton pumping was initiated by addition of NADH to 0.8 mM and terminated by addition of nigericin to 0.5 µg/mL. Fluorescence values were normalized to the maximum fluorescence after the addition of nigericin, and the percent quenching of fluorescence was determined from the minimum fluorescence value. For each experiment, 100% relative activity was defined as the percent quenching with no inhibitor present.

Computational Docking. Molecular Operating Environment (MOE; Chemical Computing Group) was used to compute docking poses for all compounds binding to AB ATP synthase. The AB ac_{10} complex was isolated from PDB 7P2Y and prepared in MOE using default settings, except that side chain protonation states were set using an external dielectric of 2 to mimic a membrane-embedded environment. MOE Site Finder was used to define the putative binding site that included cAsp60, aTrp261, and aPhe261. Ligands were prepared using MOE, including prediction of predominant protomers at pH 7. Docking poses were calculated in MOE using the AMBER10:EHT forcefield, a Born solvation model with external dielectric of 2, and induced fit refinement. Molecular graphics were prepared using PyMol (Schrödinger).

Supporting Information

ATP synthesis activity of *Acinetobacter baumannii* ISO vesicles (Figure S1), Summary of ATP synthesis and ETC Inhibition (Table S1), Inhibition of ATP synthesis activity in *Acinetobacter baumannii* (Figure S2), Inhibition of ATP synthesis activity in *Pseudomonas aeruginosa* (Figure S3), Inhibition of ATP synthesis activity by BDQ (Figure S4), Electron Transport Chain Inhibition (Figure S5), Antibacterial activity against *S. aureus* and *E. coli* (Table S2), Predicted Safety and Toxicity (Table S3), Comparison of docked WSA to BDQ binding (Figure S6), and ^{1}H and ^{13}C NMR Spectra for compounds can be found in the provide supporting information.

Conflict of Interests

The authors declare no conflict of interest.

Data Availability Statement

The data that support the findings of this study are available from the corresponding author upon reasonable request.

[1] M. Naghavi, S. E. Vollset, K. S. Ikuta, L. R. Swetschinski, A. P. Gray, E. E. Wool, G. R. Aguilar, T. Mestrovic, G. Smith, C. Han, R. L. Hsu, J. Chalek, D. T. Araki, E. Chung, C. Raggi, A. G. Hayoon, N. D. Weaver, P. A. Lindstedt, A. E. Smith, U. Altay, N. V. Bhattacharjee, K. Giannakis, F. Fell, B. McManigal, N. Ekapirat, J. A. Mendes, T. Runghien, O. Srimokla, A. Abdelkader, S. Abd-Elsalam, R. G. Aboagye, H. Abolhassani, H. Abualruz, U. Abubakar, H. J. Abukhadijah, S. Aburuz, A. Abu-Zaid, S. Achalapong, I. Y. Addo, V. Adekanmbi, T. E. Adeyeoluwa, Q. E. S. Adnani, L. A. Adzigbli, M. S. Afzal, S. Afzal, A. Agodi, A. J. Ahlstrom, A. Ahmad, S. Ahmad, T. Ahmad, A. Ahmadi, A. Ahmed, H. Ahmed, I. Ahmed, M. Ahmed, S. Ahmed, S. A. Ahmed, M. A. Akkaif, S. A. Awaidy, Y. A. Thaher, S. O. Alalalmeh, M. T. AlBataineh, W. A. Aldhaleei, A. A. S. Al-Gheethi, N. B. Alhaji, A. Ali, L. Ali, S. S. Ali, W. Ali, K. Allel, S. Al-Marwani, A. Alrawashdeh, A. Altaf, A. B. Al-Tammemi, J. A. Al-Tawfiq, K. H. Alzoubi, W. A. Al-Zyoud, B. Amos, J. H. Amuasi, R. Ancuceanu, J. R. Andrews, A. Anil, I. A. Anuoluwa, S. Anvari, A. E. Anyasodor, G. L. C. Apostol, J. Arabloo, M. Arafat, A. Y. Aravkin, D. Areda, A. Aremu, A. A. Artamonov, E. A. Ashley, M. O. Asika, S. S. Athari, M. M. W. Atout, T. Awoke, S. Azadnajafabad, J. M. Azam, S. Aziz, A. Y. Azzam, M. Babaei, F.-X. Babin, M. Badar, A. A. Baig, M. Bajcetic, S. Baker, M. Bardhan, H. J. Barqawi, Z. Basharat, A. Basiru, M. Bastard, S. Basu, N. S. Bayleyegn, M. A. Belete, O. O. Bello, A. Beloukas, J. A. Berkley, A. S. Bhagavathula, S. Bhaskar, S. S. Bhuyan, J. A. Bielicki, N. I. Briko, C. S. Brown, A. J. Browne, D. Buonsenso, Y. Bustanji, C. G. Carvalheiro, C. A. Castañeda-Orjuela, M. Cenderadewi, J. Chadwick, S. Chakraborty, R. M. Chandika, S. Chandy, V. Chansamouth, V. K. Chattu, A. A. Chaudhary, P. R. Ching, H. Chopra, F. R. Chowdhury, D.-T. Chu, M. Chutiyami, N. Cruz-Martins, A. G. da Silva, O. Dadras, X. Dai, S. D. Darcho, S. Das, F. P. D. la Hoz, D. M. Dekker, D. Diaz, B. F. R. Dickson, S. G. Djorie, M. Dodangeh, S. Dohare, K. G. Dokova, O. P. Doshi, R. K. Dowou, H. L. Dsouza, S. J. Dunachie, A. M. Dziedzic, T. Eckmanns, A. Ed-Dra, A. Eftekharimehrabad, T. C. Ekundayo, I.E. Sayed, M. Elhadi, W. El-Huneidi, C. Elias, S. J. Ellis, R. Elsheikh, I. Elsohaby, C. Eltaha, B. Eshrati, M. Eslami, D. W. Eyre, A. O. Fadaka, A. F. Fagbamigbe, A. Fahim, A. Fakhri-Demeshghieh, F. O. Fasina, M. M. Fasina, A. Fate-hizadeh, N. A. Feasey, A. Feizkhah, G. Fekadu, F. Fischer, I. Fitriana, K. M. Forrest, C. F. Rodrigues, J. E. Fuller, M. A. Gadanya, M. Gajdács, A. P. Gandhi, E. E. Garcia-Gallo, D. O. Garrett, R. K. Gautam, M. W. Gebregergis, M. Gebrehiwot, T. G. Gebremeskel, C. Geffers, L. Georgalis, R. M. Ghazy, M. Golechha, D. Golinelli, M. Gordon, S. Gulati, R. D. Gupta, S. Gupta, V. K. Gupta, A. D. Habteyohannes, S. Haller, H. Harapan, M. L. Harrison, A. I. Hasaballah, I. Hasan, R. S. Hasan, H. Hasani, A. H. Haselbeck, M. S. Hasnain, I. I. Hassan, S. Hassan, M. S. H. Z. Tabatabaei, K. Hayat, J. He, O. E. Hegazi, M. Heidari, K. Hezam, R. Holla, M. Holm, H. Hopkins, M. M. Hossain, M. Hosseinzadeh, S. Hostiuc, N. R. Hussein, L. D. Huy, E. D. Ibáñez-Prada, A. Ikiroma, I. M. Ilic, S. M. S. Islam, F. Ismail, N. E. Ismail, C. D. Iwu, C. J. Iwu-Jaja, A. Jafarzadeh, F. Jaiteh, R. J. Yengejeh, R. D. G. Jamora, J. Javidnia, T. Jawaid, A. W. J. Jenney, H. J. Jeon, M. Jokar, N. Jomehzadeh, T. Joo, N. Joseph, Z. Kamal, K. K. Kanmodi, R. S. Kantar, J. A. Kapisi, I. M. Karaye, Y. S. Khader, H. Khajuria, N. Khalid, F. Khamesipour, A. Khan, M. J. Khan, M. T. Khan, V. Khanal, F. F. Khidri, J. Khubchandani, S. Khusuwan, M. S. Kim, A. Kisa, V. A. Korshunov, F. Krapp, R. Krumkamp, M. Kuddus, M. Kulimbet, D. Kumar, E. A. P.

ChemMedChem

Research Article
doi.org/10.1002/cmdc.202400952

Chemistry Europe
European Chemical
Societies Publishing

Kumaran, A. Kuttikkattu, H. H. Kyu, I. Landires, B. K. Lawal, T. T. T. Le, I. M. Lederer, M. Lee, S. W. Lee, A. Lepape, T. L. Lerango, V. S. Ligade, C. Lim, S. S. Lim, L. W. Limenh, C. Liu, X. Liu, X. Liu, M. J. Loftus, H. I. M. Amin, K. L. Maass, S. B. Maharaj, M. A. Mahmoud, P. Maikanti-Charalampous, O. M. Makram, K. Malhotra, A. A. Malik, G. D. Mandilara, F. Marks, B. A. Martinez-Guerra, M. Martorell, H. Masoumi-Asl, A. G. Mathioudakis, J. May, T. A. McHugh, J. Meiring, H. N. Meles, A. Melese, E. B. Melese, G. Minervini, N. S. Mohamed, S. Mohammed, S. Mohan, A. H. Mokdad, L. Monasta, A. M. Ghalibaf, C. E. Moore, Y. Moradi, E. Mossialos, V. Mougin, G. D. Mukoro, F. Mulita, B. Muller-Pebody, E. Murillo-Zamora, S. Musa, P. Musicha, L. A. Musila, S. Muthupandian, A. J. Nagarajan, P. Naghavi, F. Nainu, T. S. Nair, H. H. R. Najmuldeen, Z. S. Natto, J. Nauman, B. P. Nayak, G. T. Nchanji, P. Ndishimye, I. Negoi, R. I. Negoi, S. A. Nejadghaderi, Q. P. Nguyen, E. A. Noman, D. C. Nwakanma, S. O'Brien, T. J. Ochoa, I. A. Odetokun, O. A. Ogundijo, T. R. Ojo-Akosile, S. R. Okeke, O. C. Okonji, A. T. Olagunju, A. Olivas-Martinez, A. A. Olorukooba, P. Olwoch, K. I. Onyedibe, E. Ortiz-Brizuela, O. Osuolale, P. Ounchanum, O. T. Oyeyemi, M. P. P. A, J. L. Paredes, R. R. Parikh, J. Patel, S. Patil, S. Pawar, A. Y. Peleg, P. Peprah, J. Perdigão, C. Perrone, I.-R. Petcu, K. Phommasone, Z. Z. Piracha, D. Poddighe, A. J. Pollard, R. Poluru, A. Ponce-De-Leon, J. Puvvula, F. N. Qamar, N. H. Qasim, C. D. Rafai, P. Raghav, L. Rahbarnia, F. Rahim, V. Rahimi-Movaghar, M. Rahman, M. A. Rahman, H. Ramadan, S. K. Ramasamy, P. S. Ramesh, P. W. Ramteke, R. K. Rana, U. Rani, M.-M. Rashidi, D. Rathish, S. Rattanavong, S. Rawaf, E. M. M. Redwan, L. F. Reyes, T. Roberts, J. V. Robotham, V. D. Rosenthal, A. G. Ross, N. Roy, K. E. Rudd, C. J. Sabet, B. A. Saddik, M. R. Saeb, U. Saeed, S. S. Moghaddam, W. Saengchan, M. Safaei, A. Saghazadeh, N. S. Sharif-Askari, A. Sahebkar, S. S. Sahoo, M. Sahu, M. Saki, N. Salam, S. Saleem, M. A. Saleh, Y. L. Samodra, A. M. Samy, A. Saravanan, M. Satpathy, A. E. Schumacher, M. Sedighi, S. Seekaew, M. Shafie, P. A. Shah, S. Shahid, M. J. Shahwan, S. Shakoor, N. Shalev, M. A. Shamim, M. A. Shamshirgaran, A. Shamsi, A. Sharifan, R. P. Shastry, M. Shetty, A. Shittu, S. Shrestha, E. E. Siddig, T. Sideroglou, J. Sifuentes-Osornio, L. M. L. R. Silva, E. A. F. Simões, A. J. H. Simpson, A. Singh, S. Singh, R. Sinto, S. S. M. Soliman, S. Soraneh, N. Stoesser, T. Z. Stoeva, C. K. Swain, L. Szarpak, S. S. T. Y, S. Tabatabai, C. Tabche, Z. M.-A. Taha, K.-K. Tan, N. Tasak, N. Y. Tat, A. Thaiprakong, P. Thangaraju, C. C. Tigoi, K. Tiwari, M. R. Tovani-Palone, T. H. Tran, M. Tumurkhuu, P. Turner, A. J. Udoakang, A. Udoh, N. Ullah, S. Ullah, A. G. Vaithinathan, M. Valenti, T. Vos, H. T. L. Vu, Y. Waheed, A. S. Walker, J. L. Walson, T. Wangrangsimakul, K. G. Weerakoon, H. F. L. Wertheim, P. C. M. Williams, A. A. Wolde, T. M. Wozniak, F. Wu, Z. Wu, M. K. K. Yadav, S. Yaghoubi, Z. S. Yahaya, A. Yarahmadi, S. Yezli, Y. E. Yismaw, D. K. Yon, C.-W. Yuan, H. Yusuf, F. Zakham, G. Zamagni, H. Zhang, Z.-J. Zhang, M. Zielińska, A. Zumla, S. H. H. Zyoud, S. H. Zyoud, S. I. Hay, A. Stergachis, B. Sartorius, B. S. Cooper, C. Dolecek, C. J. L. Murray, *The Lancet* **2024**, *404*, 1199–1226, DOI 10.1016/S0140-6736(24)-01867-1.

[2] Centers for Disease Control and Prevention, *HAI Pathogens and Antimicrobial Resistance Report, 2018–2021*, U.S. Department Of Health And Human Services, CDC, **2023**.

[3] Centers for Disease Control and Prevention (U.S.), *Antibiotic Resistance Threats in the United States, 2019*, Centers For Disease Control And Prevention (U.S.), **2019**.

[4] R. Vivas, A. A. T. Barbosa, S. S. Dolabela, S. Jain, *Microbial Drug Resistance* **2019**, *25*, 890–908.

[5] I. Kyriakidis, E. Vasileiou, Z. D. Pana, A. Tragiannidis, *Pathogens* **2021**, *10*, 373.

[6] A. Gauba, K. M. Rahman, *Antibiotics* **2023**, *12*, 1590.

[7] K. Hards, G. M. Cook, *Drug Resistance Updates* **2018**, *36*, 1–12.

[8] M. Donnert, S. Elsheikh, A. Arce-Rodriguez, V. Pawar, P. Braubach, D. Jonigk, A. Haverich, S. Weiss, M. Müsken, S. Häussler, *PLoS Pathog* **2020**, *16*, e1009126.

[9] A. Nemec, in *Bergey's Manual of Systematics of Archaea and Bacteria*, John Wiley & Sons, Ltd, **2022**, pp. 1–78.

[10] J. Bai, Y. Dai, A. Farinha, A. Y. Tang, S. Syal, G. Vargas-Cuebas, T. van Opijnen, R. R. Isberg, E. Geisinger, *Journal of Bacteriology* **2021**, *203*, 10.1128/jb.00565-20.

[11] N. R. Glasser, S. E. Kern, D. K. Newman, *Molecular Microbiology* **2014**, *92*, 399–412.

[12] B. E. Poulsen, R. Yang, A. E. Clatworthy, T. White, S. J. Osmulski, L. Li, C. Penaranda, E. S. Lander, N. Shoresh, D. T. Hung, *Proceedings of the National Academy of Sciences* **2019**, *116*, 10072–10080.

[13] W. Kühlbrandt, *Annu. Rev. Biochem.* **2019**, *88*, 515–549.

[14] K. Andries, P. Verhasselt, J. Guillemont, H. W. H. Göhlmann, J.-M. Neefs, H. Winkler, J. Van Gestel, P. Timmerman, M. Zhu, E. Lee, P. Williams, D. de Chaffoy, E. Huitric, S. Hoffner, E. Cambau, C. Truffot-Pernot, N. Lounis, V. Jarlier, *Science* **2005**, *307*, 223–227.

[15] H. Guo, G. M. Courbon, S. A. Bueler, J. Mai, J. Liu, J. L. Rubinstein, *Nature* **2021**, *589*, 143–147.

[16] J. K. Demmer, B. P. Phillips, O. L. Uhrig, A. Filloux, L. P. Allsopp, M. Bublitz, T. Meier, *Science Advances* **2022**, *8*, eabl5966.

[17] J. F. Ciprich, A. J. E. Buckhalt, L. L. Carroll, D. Chen, S. A. DeFiglia, R. S. McConnell, D. J. Parmar, O. L. Pistor, A. B. Rao, M. L. Rubin, G. E. Volk, P. R. Steed, A. L. Wolfe, *ACS Omega* **2022**, *7*, 28434–28444.

[18] V. M. Fraunfelter, B. A. Pugh, A. P. L. Williams, K. T. Ward, D. O. Jackson, M. Austin, J. F. Ciprich, L. Dippy, J. Dunford, G. N. Edwards, E. Glass, K. M. Handy, C. N. Kellogg, K. Llewellyn, K. Q. Nyberg, S. J. Shepard, C. Thomas, A. L. Wolfe, P. R. Steed, *ACS Infect. Dis.* **2023**, *9*, 2448–2456, DOI 10.1021/acsinfecdis.3c00317.

[19] K. T. Ward, A. P. L. Williams, C. A. Blair, A. M. Chatterjee, A. Karthikeyan, A. S. Roper, C. N. Kellogg, P. R. Steed, A. L. Wolfe, *ACS Med. Chem. Lett.* **2023**, *15*, 149–155, DOI 10.1021/acsmedchemlett.3c00480.

[20] E. J. Geddes, M. K. Gugger, A. Garcia, M. G. Chavez, M. R. Lee, S. J. Perlmutter, C. Bieniossek, L. Guasch, P. J. Hergenrother, *Nature* **2023**, *624*, 145–153.

[21] M. Bashir, M. Arshad, R. Begum, V. K. Aggarwal, *Org Lett* **2023**, *25*, 4281–4285.

[22] L. Preiss, J. D. Langer, Ö. Yildiz, L. Eckhardt-Strelau, J. E. G. Guillemont, A. Koul, T. Meier, *Sci. Adv.* **2015**, *1*, e1500106.

[23] C. Adolph, C.-Y. Cheung, M. B. McNeil, W. J. Jowsey, Z. C. Williams, K. Hards, L. K. Harold, A. Aboelela, R. S. Bujaroski, B. J. Buckley, J. D. A. Tyndall, Z. Li, J. D. Langer, L. Preiss, T. Meier, A. J. C. Steyn, K. Y. Rhee, M. Berney, M. J. Kelso, G. M. Cook, *Cell Chem. Biol.* **2023**, *31*, 683–688.

[24] H. C. Tien, A. Battad, E. A. Bryce, J. Fuller, M. Mulvey, K. Bernard, R. Brisebois, J. J. Doucet, S. B. Rizoli, R. Fowler, A. Simor, *BMC Infect Dis.* **2007**, *7*, 95.

[25] J. L. Burns, J. Emerson, J. R. Stapp, D. L. Yim, J. Krzewinski, L. Louden, B. W. Ramsey, C. R. Clausen, *Clin Infect Dis* **1998**, *27*, 158–163.

[26] R. H. Fillingame, *J Bacteriol* **1975**, *124*, 870–883.